Penerbit Akademia Baru

Journal of Advanced Research Design

Journal homepage:
https://akademiabaru.com/submit/index.php/ard
ISSN: 2289-7984

GCPV-DSTATCOM Performance Analysis with PQ Theory and HCGBP Control Algorithm under Unbalanced Load Conditions

Muhammad Ariff Haikal Ridzwan[1], Nor Hanisah Baharudin[1,2,*], Tunku Muhammad Nizar Tunku Mansur[1,2], Rosnazri Ali[1,2], Mohd Syahril Noor Shah[1,2], Kumuthawathe Ananda-Rao[1,2]

[1] Department of Electrical Engineering, Faculty of Electrical Engineering & Technology, University of Malaysia Perlis, 06200 Arau, Perlis, Malaysia
[2] Centre of Excellence for Renewable Energy (CERE), Faculty of Electrical Engineering & Technology, Universiti Malaysia Perlis, Pauh Putra Campus, 02600 Arau, Perlis, Malaysia

ARTICLE INFO

Article history:
Received 2 February 2025
Received in revised form 1 September 2025
Accepted 23 September 2025
Available online 1 October 2025

Keywords:
Solar Photovoltaic; DSTATCOM; Neural Network

ABSTRACT

This paper investigates the performance of a grid-connected solar photovoltaic (GCPV) based Distribution Static Compensator (DSTATCOM) with a hybrid conjugate gradient backpropagation (HCGBP) controller. The study introduces a hybrid control algorithm that combines Instantaneous Reactive Power Theory with conjugate gradient backpropagation neural network for a three-phase, three-wire grid-connected solar PV (GCPV) based DSTATCOM. The proposed system is implemented in a simulation environment using MATLAB/Simulink. The system's performance is evaluated under two conditions: non-linear steady-state and load balancing conditions. The results indicate that the proposed control algorithm significantly reduces the Total Harmonic Distortion (THD) of the line current, achieving THD values of 1.32% and 1.33% under both conditions, compared to the THD reduction of 4.56% achievable with the PQ Theory alone under the same conditions. This demonstrates the effectiveness of the HCGBP control strategy, offering improved efficiency, faster response, and ease of implementation. Moreover, the simulation outcomes validate the reduction of THD in the line current at the Point of Common Coupling (PCC) has been successfully decreased to below 8%, aligning with the IEEE standard 519:2014.

1. Introduction

1.1 Research Background

In recent times, renewable energy sources are receiving significant attention and backing, driven by a range of factors, including political incentives and government initiatives. These sustainable energy sources encompass wind, solar, geothermal, and other alternatives [1]. Among renewable energy sources, solar photovoltaic (PV) systems have emerged as the major means of electricity generation, primarily due to their numerous advantages. These systems produce electricity directly from solar energy through the use of photovoltaic cells. PV cells offer a straightforward method of

* *Corresponding author.*
E-mail address: norhanisah@unimap.edu.my

https://doi.org/10.37934/ard.143.1.231247

power generation as they lack moving components, demand minimal maintenance, and boast a cost-effective operational profile compared to alternative electricity sources. Furthermore, they exhibit a prolonged lifespan, produce no pollution during operation, and can be easily installed in any location with access to sunlight [2]. Grid-connected photovoltaic (PV) generators are witnessing a surge in popularity due to their consistent performance and their capability to harness power from renewable sources. These PV arrays are linked to a DC/DC boost converter, which optimizes the energy output to harness the maximum potential of the PV arrays.

The photovoltaic (PV) system is then connected to a DC/AC voltage source converter (VSC) in order to transmit electrical energy to the AC power grid [3], [4]. Because the electricity generated by the PV array cannot be seamlessly incorporated into the grid and loads, a voltage source converter (VSC) is employed as a power converter. When solar PV are connected to the utility grid, the rapid utilization of nonlinear loads like rectifiers can introduce harmonic currents into the distribution system [5]–[7].

The issues related to power quality in the distribution system are of significant concern due to their adverse effects on both the equipment of the load and the utility system [8]–[10]. To address these power quality concerns, voltage source converters (VSCs) are employed as distribution static compensators (DSTATCOMs), which improve power factor and reduce harmonics. However, the effectiveness of DSTATCOMs relies on the control algorithm used for estimating current references and generating gating pulses. Therefore, the development and implementation of a control algorithm should prioritize characteristics such as better convergence, adaptability, low computational complexity, and ease of application. To achieve these objectives, various control techniques like PQ theory, synchronous reference frame (SRF) theory , instantaneous symmetrical control (ISC) theory, and average unit power factor (AUPF) theory are frequently employed in the design of DSTATCOM systems [11], [12].

As a result, there is a growing need for control algorithms that offer improved convergence and adaptability, reduced computational complexity, and ease of implementation. To address these requirements, neural network (NN) control algorithms are increasingly employed, leveraging their intricate neural structure and improved accuracy in assessment. Consequently, neural network-based control techniques are being used more frequently for rapid harmonic analysis and detection. This approach offers several advantages, including enhanced reliability, energy efficiency, and improved performance, all without necessitating significant hardware modifications. When addressing power quality issues, the neural network-based control technique incorporating gradient descent with momentum has demonstrated its effectiveness in alleviating uncertainties, nonlinearities, and harmonics, ultimately delivering a suitable and responsive solution [5].

1.2 Control Algorithm

The controller's role in generating reference current signals is pivotal for mitigating power quality issues and ensuring the optimal performance of a DSTATCOM. Various control strategies, including Instantaneous Reactive Power (IRP) theory, Discrete Fourier Transform, Synchronous Reference Frame (SRF) Theory, and Wavelet Transform, can be employed to generate these reference current signals. Among these control strategies, the PQ theory stands out as the most efficient and effective approach in addressing power quality concerns. DSTATCOM, equipped with Voltage Source Converter (VSC), helps neutralize the inherent current of the power source. To maintain the consistency of the DSTATCOM's DC link voltage, a DC voltage regulator is employed [13].

The utilization of Instantaneous Power Theory has yielded excellent results in the design of a Distribution Static Compensator (DSTATCOM) [14]. The combination of PV-DSTATCOM, however, has

been a relatively recent development that has evolved over the past several years [15]. This system has the capability to simultaneously enhance power factor, rectify current imbalances, and mitigate current harmonics as well as injecting PV-generated energy into the grid with minimal total harmonic distortion (THD). Furthermore, even in the absence of electricity generation from PV, the system can contribute to enhancing the overall power quality of the utility grid. Based on current understanding, the pioneering concept was initially introduced by Kim and others in 1996 [3], [16].

1.2.1 PQ theory Control Algorithm

The control algorithm known as Instantaneous Reactive Power (IRP) theory, which was introduced by Akagi, is also commonly referred to as the PQ Theory. Through Clark's transformation, the PQ Theory is able to convert the measured three-phase voltage and load currents into two-phase quantities within the *α-β* frame. This theory also enables the conversion of active and reactive power into this same frame [17], [18]. Subsequently, the reference currents within the *α-β* frame can be converted back into the *abc* frame using the reverse Clark's transformation. Clark's transformation is also used to convert the line voltages V_a, V_b, and V_c, as well as the load currents I_{La}, I_{Lb}, and I_{Lc}, into the α-β frame. Equation (1) until (5) represents the set of equations used in the P-Q theory control algorithm. These equations are utilized to calculate the control signals for managing active and reactive power flow in electrical systems.

$$\begin{bmatrix} V_0 \\ V_\alpha \\ V_\beta \end{bmatrix} = \sqrt{\frac{2}{3}} \begin{bmatrix} 1/\sqrt{2} & 1/\sqrt{2} & 1/\sqrt{2} \\ 1 & -1/2 & -1/2 \\ 0 & \sqrt{3}/2 & -\sqrt{3}/2 \end{bmatrix} \begin{bmatrix} V_a \\ V_b \\ V_c \end{bmatrix} \quad (1)$$

$$\begin{bmatrix} I_0 \\ I_\alpha \\ I_\beta \end{bmatrix} = \sqrt{\frac{2}{3}} \begin{bmatrix} 1/\sqrt{2} & 1/\sqrt{2} & 1/\sqrt{2} \\ 1 & -1/2 & -1/2 \\ 0 & \sqrt{3}/2 & -\sqrt{3}/2 \end{bmatrix} \begin{bmatrix} I_{La} \\ I_{Lb} \\ I_{Lc} \end{bmatrix} \quad (2)$$

The active and reactive powers at a specific moment are expressed as follows:

$$\begin{bmatrix} P \\ Q \end{bmatrix} = \begin{bmatrix} V_\alpha & V_\beta \\ -V_\beta & V_\alpha \end{bmatrix} \begin{bmatrix} I_\alpha \\ I_\beta \end{bmatrix} \quad (3)$$

Average $(\bar{p})$ and oscillatory $(\tilde{p})$ is the result of instantaneous active and reactive power p and q after being decomposed. In order to counterbalance the oscillating part of the momentary active power, the reference source currents in *I*α* and *I*β* are determined using the following equation.

:

$$\begin{bmatrix} I^*_\alpha \\ I^*_\beta \end{bmatrix} = \frac{1}{\Delta} \begin{bmatrix} V_\alpha & -V_\alpha \\ V_\beta & V_\beta \end{bmatrix} \begin{bmatrix} \bar{P} \\ 0 \end{bmatrix} \quad (4)$$

Where $\Delta = V_\alpha^2 + V_\beta^2$. To compute the reference source currents in the *abc* frame from the reference source currents in the *α-β* frame, the inverse Clark's transformation is employed, and it is expressed as follows:

$$\begin{bmatrix} I*_a \\ I*_b \\ I*_c \end{bmatrix} = \sqrt{\frac{2}{3}} \begin{bmatrix} 1/\sqrt{2} & 1 & 0 \\ 1/\sqrt{2} & -1/2 & \sqrt{3}/2 \\ 1/\sqrt{2} & -1/2 & -\sqrt{3}/2 \end{bmatrix} \begin{bmatrix} I*_0 \\ I*_\alpha \\ I*_\beta \end{bmatrix} \quad (5)$$

1.2.2 Backpropagation neural network

BPNN, or Back-Propagation Neural Network is recognized as a feedforward network featuring a multilayer perceptron (MLP) architecture. It derives its name from the error back-propagation technique, which was introduced in 1986. The fundamental MLP typically comprises three layers: an input layer, a hidden layer, and an output layer. Additional hidden layers can be incorporated, and the number of hidden layers is a tuneable parameter that should be explicitly adjusted [19].

The sample BPNN in **Error! Reference source not found.** comprises two HLs, each having three and four neurons. The details of a single HL neuron's operation are provided. For example, equation (6) can express an HL neuron's output Y if it accepts n input data [19].

$$Y = F_{ACT}\left(\sum_{j=1}^{n} w_j X_j + b\right) \quad (6)$$

In the context of neural networks, *Xj* represents the *jth* input data, *wj* signifies its weight value, *b* denotes the bias value, and *Fact* is the activation function. The activation function is responsible for introducing nonlinearity into the network, and two widely used activation functions are the sigmoid and hyperbolic tangent (*tanh*) functions [19].

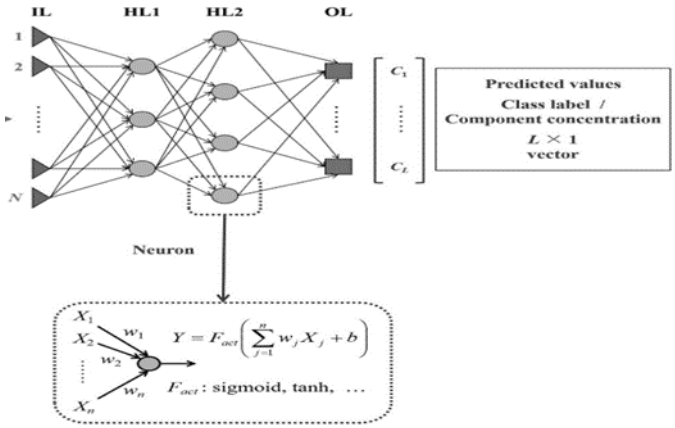

Fig.1. Processing Data for BPNN [19]

2.Methodology

2.1 DSTATCOM Configuration

The DSTATCOM, known as a custom power device, is connected with the existing system in parallel. Its primary purpose is to effectively manage and rectify issues related to electrical current and power quality, thus enhancing the overall electrical system performance [20]. DSTATCOM is a device that is essential for mitigating harmonic currents, compensating for reactive currents, and balancing loads in AC distribution systems. It also functions as a voltage source converter (VSC) comprising semiconductor valves, self-communication capabilities, and capacitors on the DC bus. In

general, DSTATCOM can offer power factor correction, harmonic compensation, and load balancing. However, when compared to the conventional static VAR compensator (SVC), DSTATCOM offers the advantages of being able to provide rated current at almost any network voltage, delivering improved dynamic response, and requiring smaller capacitors on the DC bus [21].

The VSC is an essential component in determining the performance of a DSTATCOM. The DSTATCOM is typically connected to all three AC main phases and three non-linear phases. To reduce current ripple, the VSC's AC output is connected to an interfacing inductor (L_f) [22]. **Fig. 1** depicts a schematic diagram illustrating a three-phase AC supply connected in series with a source impedance (Zs). This series connection is then linked to a non-linear load consisting of a rectifier and an RL load. Ultimately, the interconnected AC supply and non-linear load are in parallel with a DSTATCOM that includes six IGBTs.

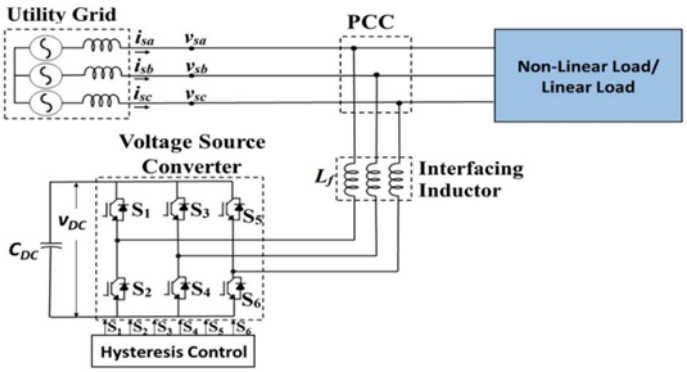

Fig. 1 Three Phase Three Wire DSTATCOM Schematic Diagram

2.1.1 Selecting the DC bus voltage (VDC)

The magnitude of the DC bus voltage (V_{DC}) in a VSC based DSTATCOM primarily relies on the instantaneous energy available to the DSTATCOM. To effectively implement Pulse Width Modulation (PWM) control in a VSI-based DSTATCOM and prevent issues such as current distortion and exceeding current limits, it is crucial for the DC bus voltage (VDC) to be at least twice the magnitude of the AC mains voltage [23]. "Furthermore, it is essential that the minimum DC bus voltage value exceeds the peak of the phase voltage of the system to prevent current distortion.

The minimum dc bus voltage value can be calculated by using Equation (7).

$$V_{dc} = \frac{2\sqrt{2}V_{LL}}{\sqrt{3}m} \tag{7}$$

Where, Output AC Line Voltage from the DSTATCOM, $V_{LL,}$ = 415 V, Modulation index, m = 1

2.1.2 Selecting the DC bus capacitor (C_{DC})

The value of the DC bus capacitance (CDC) is determined by both the power requirements and the desired level of DC bus voltage. As such, it can be calculated by applying the principle of energy conversion. Equation (8) shows the formula used to calculate C_{DC} [24][25].

$$\frac{1}{2} \times C_{DC} \times (V_{DC1}^2 - V_{DC2}^2) = k_1 \times 3 \times V \times a \times I \times t \quad (8)$$

Where, average DC bus voltage V_{DC1} = 700 V, The lowest required value of DC bus voltage, V_{DC2} = 677.69 V, Variation of energy during dynamics, k_1 = 10% = 0.1, Phase voltage, V = 239.60 V, Overloading factor, a = 1.2, Phase current, I = 76.2 A, Time for the DC bus voltage to recover, t = 30 ms.

2.1.3 Selecting the Interfacing AC Inductor (L_f)

The choice of the AC inductance (L_f) is contingent on factors such as the current ripple ($i_{cr(p\text{-}p)}$), switching frequency (f_s), and DC bus voltage (V_{DC}). The formula for L_f is defined as Equation (9), where the modulation index is represented as 'm' and the overload factor is denoted as 'a' [26].

$$L_f = \frac{(\sqrt{3} m\, V_{DC})}{(12 a f_s i_{cr,(p-p)})} \quad (9)$$

By considering $i_{cr,pp}$ = 15%, f_s= 1.8 kHz, m=1, V_{DC} =700 V, and a =1.2, the value of L_f is calculated to be 4 mH. The round-off value of 4mH is selected in this investigation.

2.2 Neural Network Configuration

In this research paper, an advanced performance enhancement technique for the DSTATCOM is presented. This technique involving the implementation of a neural network-based control algorithm based on the P-Q theory. **Fig. 2**. illustrates the block diagram of the proposed neural network-based P-Q theory for a three-phase, three-wire DSTATCOM. In order to enhance the performance of the P-Q control, the calculated Ploss will be filtered and generated by a neural network in NN1. A similar approach will be applied to the calculated PDC, which will be filtered and generated by a neural network in NN2 [27]. The P_{loss} and P_{DC} values generated by the neural network will be employed to calculate the current references, and these calculated current references will then be utilized in the hysteresis control strategy.

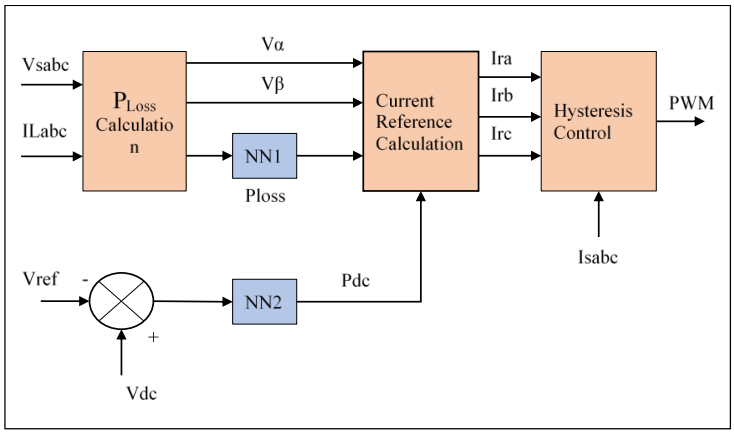

Fig. 2. Block diagram depicting the neural network-based implementation of the proposed P-Q theory

Error! Reference source not found. provides an overview of the parameters used for the neural networks, which comprise three layers: an input layer featuring a single input neuron, a hidden layer with 10 hidden neurons, and an output layer with a solitary output neuron. The hidden layer's function plays a significant role in the learning process of the neural network. The choice of having 10 hidden neurons in the hidden layer is somewhat arbitrary but is made with the aim of enhancing the system's performance [28]. The number of hidden layers and neurons in each layer are contingent upon the problem complexity being addressed. These choices are often made to accommodate the specific characteristics and requirements of the problem at hand [29].

Table 1
Neural Networks Parameters for Training in MATLAB

Parameter	Value	
	NN1	**NN2**
Number of Training Data	700	700
Number of Testing Data	150	150
Number of Neurons in Input Layer	1	1
Number of Neurons in Hidden Layer	10	10
Training Function	Scaled Conjugate Gradient	Scaled Conjugate Gradient
Performance Function	Mean squared error (MSE)	Mean squared error (MSE)
Maximum Epoch	1000	1000

3. Result and Discussion

3.1 Performance of GCPV-DSTATCOM based PQ Theory under Non-Linear Load in Steady-State Condition

Fig. 3 and **Fig. 4** illustrate the performance of the developed three-phase, three-wire Grid-Connected Photovoltaic with DSTATCOM (GCPV-DSTATCOM) based on the P-Q theory system under non-linear loads. In **Fig. 3** (a), waveform analysis is presented for line current, load current, and compensation current, while **Fig. 3** (b) displays the waveform analysis for line voltage, load voltage, and DC link voltage (V_{DC}).

In **Fig. 3** (a), it is observed that the waveform generated by the Line Current is sinusoidal, whereas the Load Current exhibits a distorted waveform. **Fig. 4** shows the waveform and Fast Fourier Transform (FFT) analysis for GCPV under linear load during steady-state conditions. **Table 2** provides the Total Harmonic Distortion (THD) values for Line Current, which are measured at 4.62%, 4.58%, and 4.56% for Phases A, B, and C, respectively. These THD values align with the limits specified by the IEEE-519:2014 standard, which mandates a THD of less than 5% for line currents.

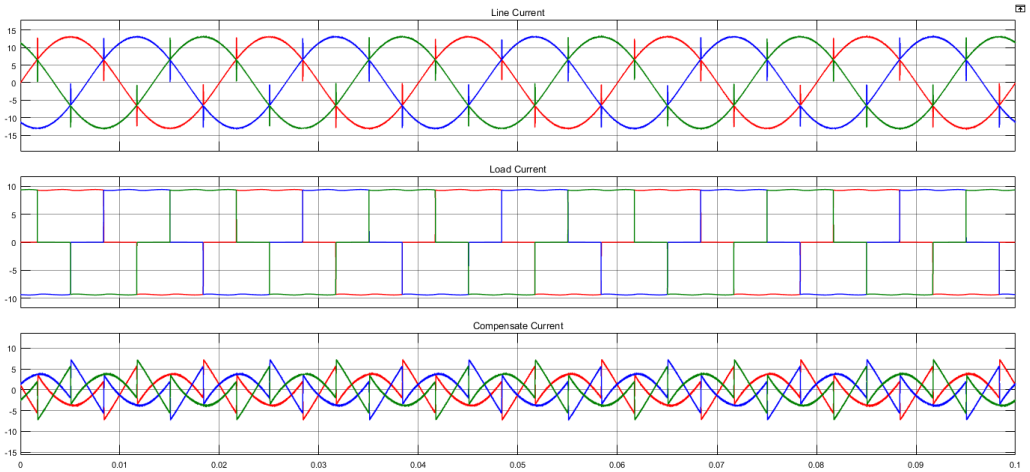

(a)

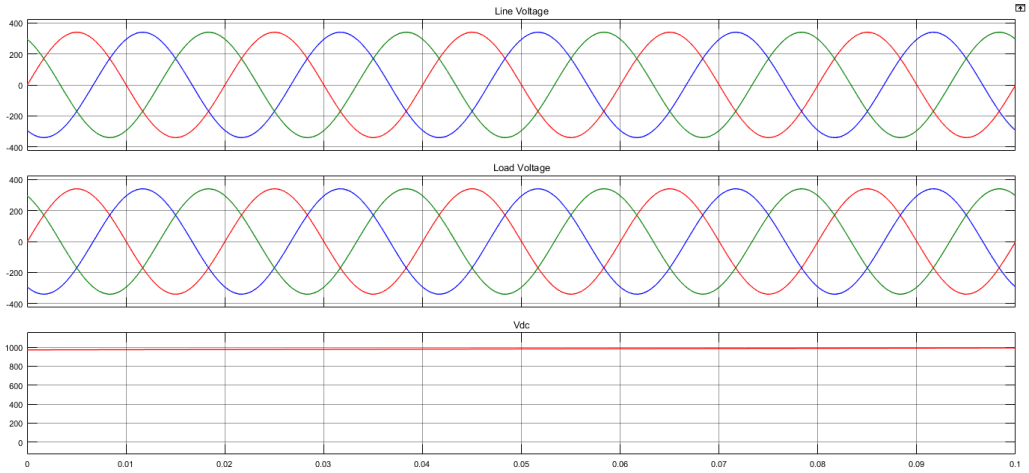

(b)

Fig. 3 Waveform analysis of GCPV-DSTATCOM based PQ Theory under Non-linear Load in Steady-State Condition (a) Line Current, Load Current, and Compensation Current, (b) Line Voltage, Load Voltage, and DC link Voltage

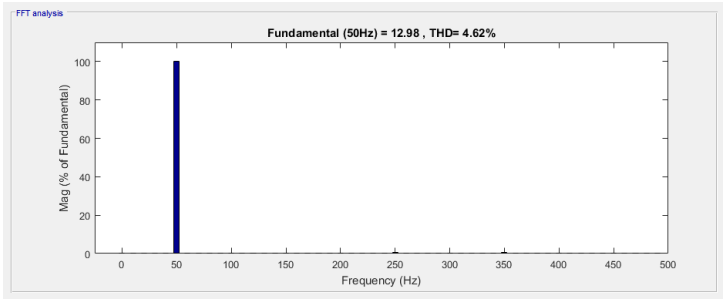

(a)

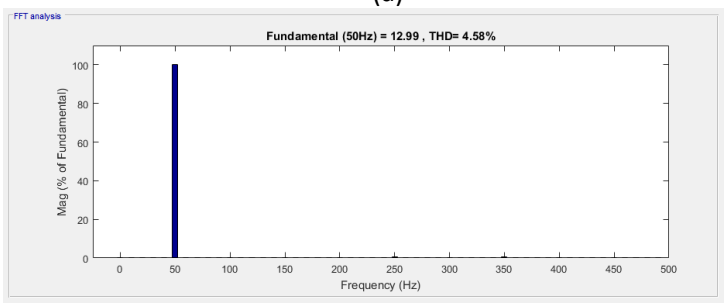

(b)

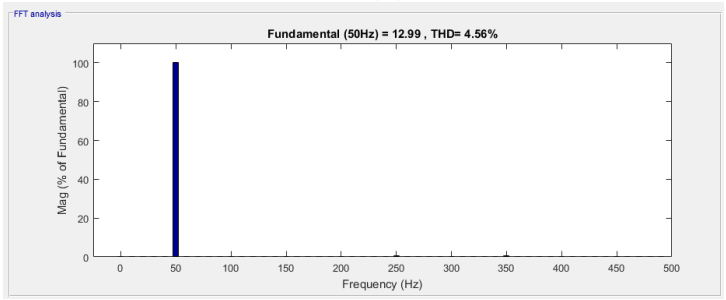

(c)

Fig. 4. Waveform and FFT Analysis for Line Current (a) Phase A, (b) Phase B, (c) Phase C

Table 2
THD Analysis for GCPV-DSTATCOM based PQ Theory under Non-Linear Load in Steady State Condition

Phase	THD (%)	
	Line Current	Load Current
Phase A	4.62	30.83
Phase B	4.58	30.83
Phase C	4.56	30.82

3.2 Performance of GCPV-DSTATCOM based PQ Theory under Non-Linear Load in Load Balancing Condition

Fig. 5 (a) presents the waveform of the load current when the load from Phase A was disconnected between 0 and 0.5 seconds. The results show that when Phase A is disconnected, the load current drops to zero for that duration. In **Fig. 5** (b), the waveforms of the line and compensation currents during the Phase A disconnection are displayed. The results indicate that the disconnection of Phase A has a noticeable impact on the shape of the line and compensation current waveforms both before and after the disconnection. For Phases B and C, the disconnection significantly affects the waveform amplitude and shape before 0.5 seconds.

Fig.6 and

Table 3 provide the waveform and Fast Fourier Transform (FFT) analysis for the line current during load balancing, with Phase A's load being disconnected. The analysis demonstrates that the Total Harmonic Distortion (THD) values for Phase A, B, and C are 4.62%, 4.58%, and 4.56%, respectively, all of which are well within the limits specified by the IEEE-519 standard for all phases. This analysis shows that the proposed DSTATCOM capable to reduce harmonic even in load balancing condition.

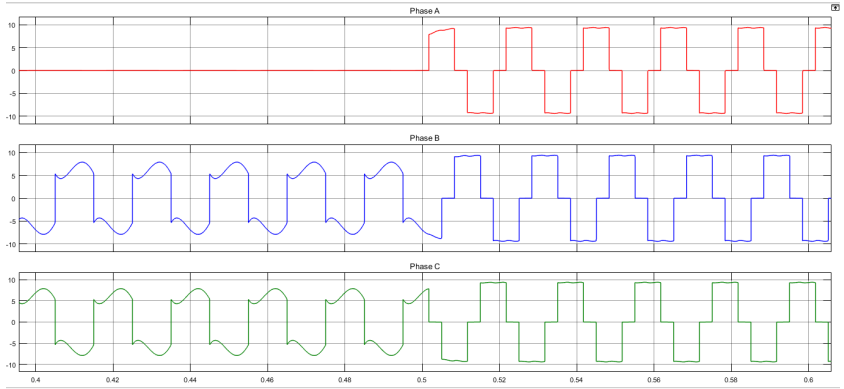

(a)

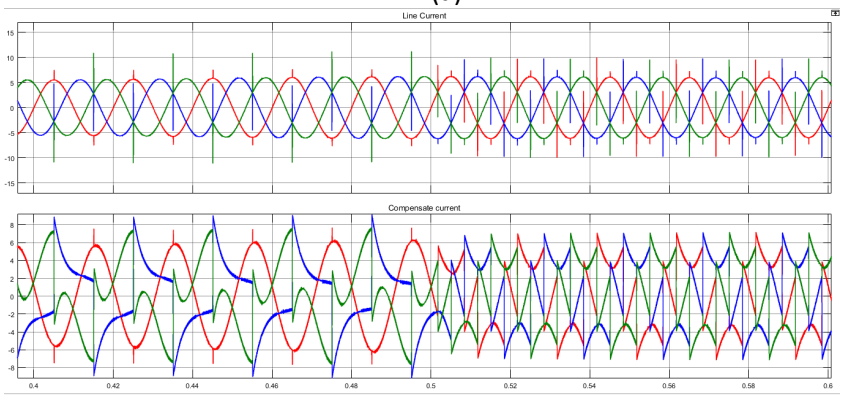

(b)

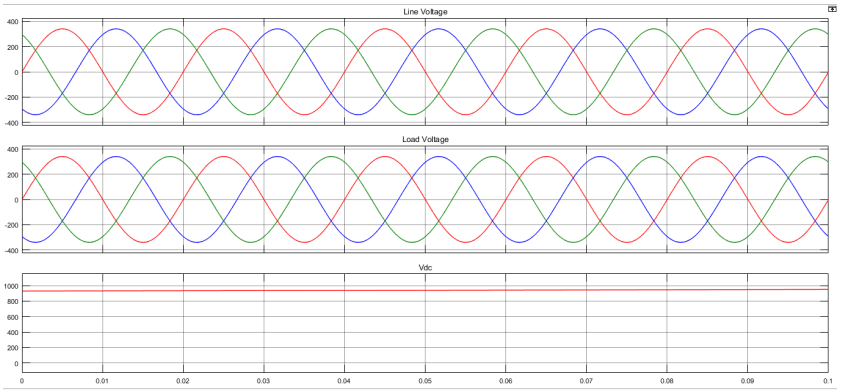

(c)

Fig. 5. Waveform analysis of GCPV-DSTATCOM based PQ Theory under Non-linear Load in Load Balancing Condition (a) Line Current, Load Current, and Compensation Current, (b) Line Voltage, Load Voltage, and DC link Voltage

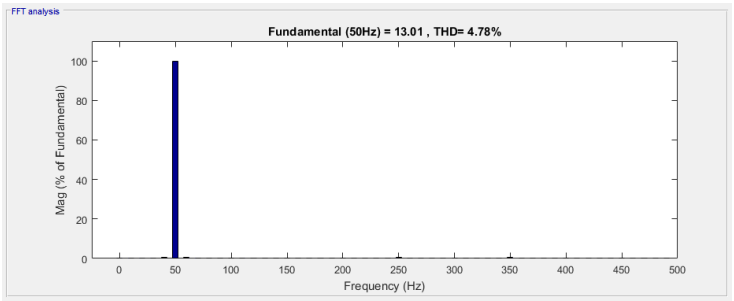

(a)

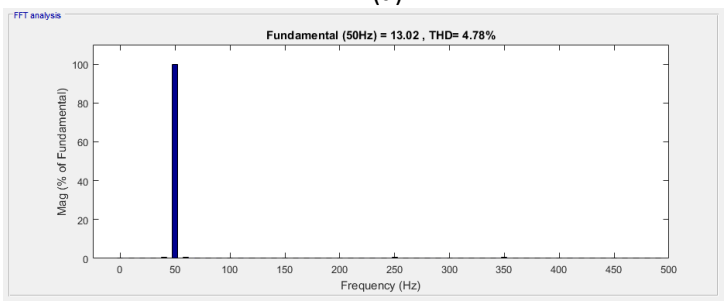

(b)

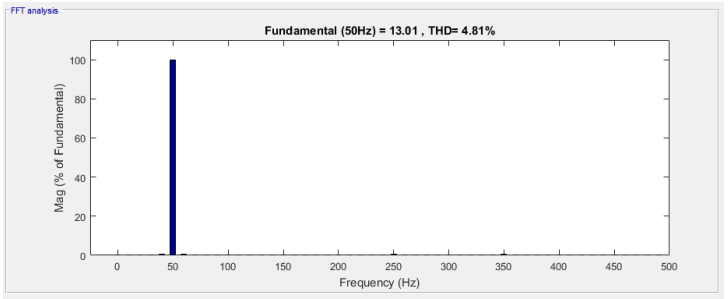

(c)

Fig.6. Waveform and FFT Analysis for Line Current (a) Phase A, (b) Phase B, and (c) Phase C

Table 3
THD Analysis for GCPV-DSTATCOM based PQ Theory under Non-Linear Load in Load Balancing Condition

Phase	THD (%)	
	Line Current	Load Current
Phase A	4.62	30.83
Phase B	4.58	30.83
Phase C	4.56	30.82

3.3 Performance of GCPV-DSTATCOM based HCGBP under Non-Linear Load in Steady-State Condition

The analysis for this simulation includes an assessment of the shape of waveform for line and load currents, along with the Total Harmonic Distortion (THD) values. **Fig.7** and **Fig.8** present the results recorded after the simulation. In **Fig.7** (a), the waveforms for Line Current, Load Current, and Compensation Current are displayed, while **Fig.7** (b) shows Line Voltage, Load Voltage, and DC Link Voltage (V_{DC}). The results indicate that the waveforms generated by line current and load in **Fig.7** (a) are sinusoidal.

Furthermore, **Fig.8** provides the waveforms and Fast Fourier Transform (FFT) analysis for GCPV under linear load during steady-state conditions. **Table 4** reveals that the THD values for Line Current are measured at 1.32%, 1.34%, and 1.34% for Phases A, B, and C, respectively. These THD values align with the IEEE-519:2014 standard, which specifies a THD of less than 5% for line currents. This analysis also shows that the proposed HCGBP has better performance than normal PQ theory in mitigating harmonic for line current at PCC.

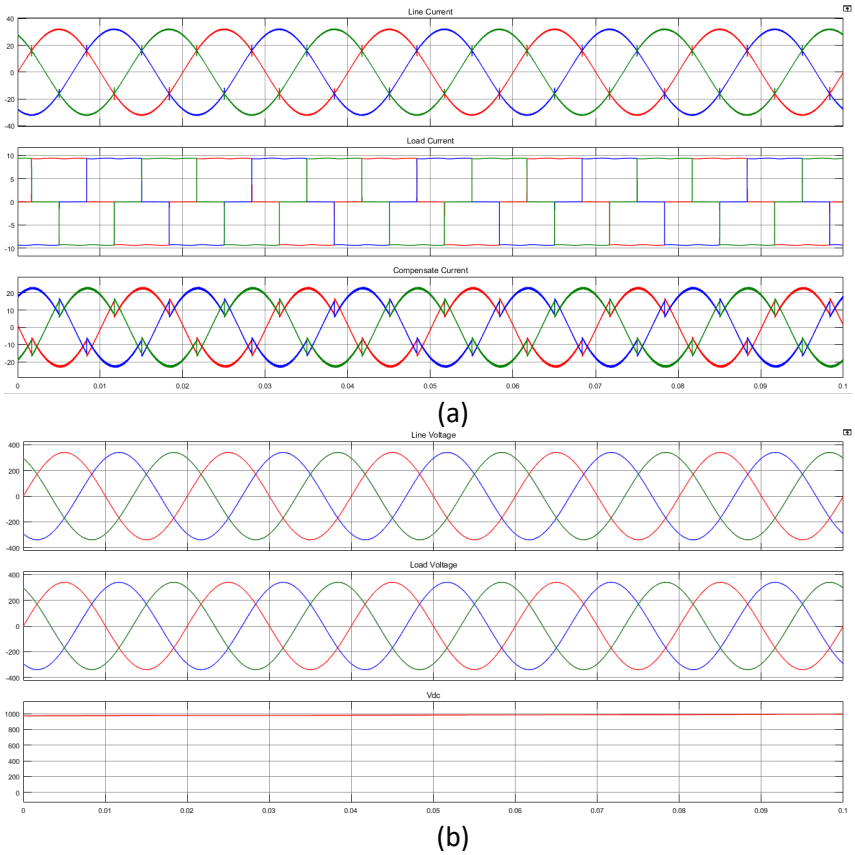

Fig.7. Waveform analysis of GCPV-DSTATCOM based HCGBP under Non-linear Load in Steady-State Condition (a) Line Current, Load Current, and Compensation Current, (b) Line Voltage, Load Voltage, and DC link Voltage

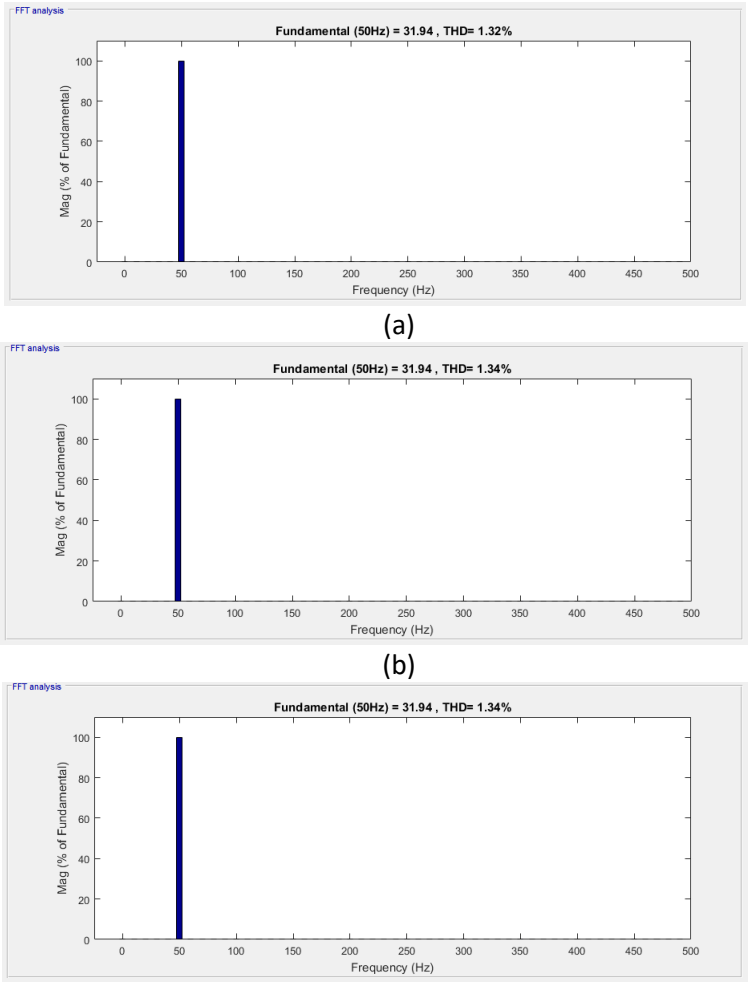

Fig.8. Waveform and FFT Analysis for Line Current (a) Phase A, (b) Phase B, and (c) Phase C

Table 4
THD Analysis for GCPV-DSTATCOM based HCGBP under Non-Linear Load in Steady State Condition

Phase	THD (%)	
	Line Current	Load Current
Phase A	1.32	30.87
Phase B	1.34	30.86
Phase C	1.34	30.87

3.4 Performance of GCPV-DSTATCOM based HCGBP under Non-Linear Load in Load Balancing Condition

Fig.9 presents the analysis of the High Capacity Grid Battery (HCGB) with GCPV Linear Load when Phase A was disconnected from 0 to 0.5 seconds. The analysis includes an examination of the effect on line current Total Harmonic Distortion (THD) values when one of the phase loads is disconnected.

In **Fig.9** (a), the load current waveform during the disconnection of Phase A is shown. The results demonstrate that when Phase A is disconnected, the load current drops to zero for that period. In **Fig.9** (b), the waveforms of the line and compensation currents during the disconnection of Phase A are displayed. The results indicate that the disconnection of Phase A has a notable impact on the

shape of the line and compensation current waveforms both before and after the disconnection. For Phases B and C, the disconnection significantly affects the waveform amplitude and shape before 0.5 seconds.

Fig.10 and **Table 5** provide the waveform and Fast Fourier Transform (FFT) analysis for line current during load balancing, with Phase A's load being disconnected. The analysis reveals that the THD value for Phase A is 1.34%, while the THD values for Phases B and C are both 1.33%. These THD values comply with the IEEE-519:2014 standard, which specifies a THD of less than 5% for line currents. This indicates that load balancing does not significantly affect the THD value in a non-linear load.

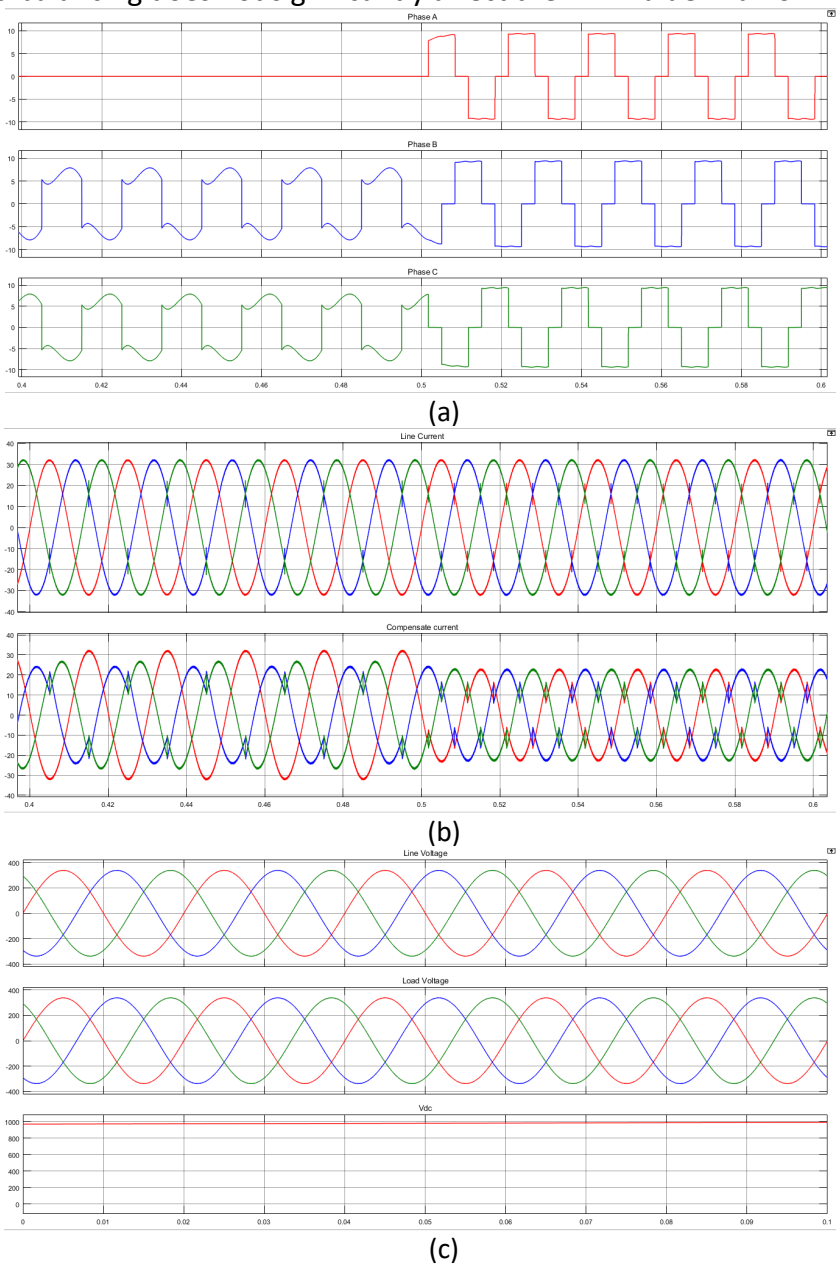

Fig.9. Waveform analysis of GCPV-DSTATCOM based PQ Theory under Non-linear Load in Load Balancing Condition (a) Line Current, Load Current, and Compensation Current, (b) Line Voltage, Load Voltage, and DC link Voltage

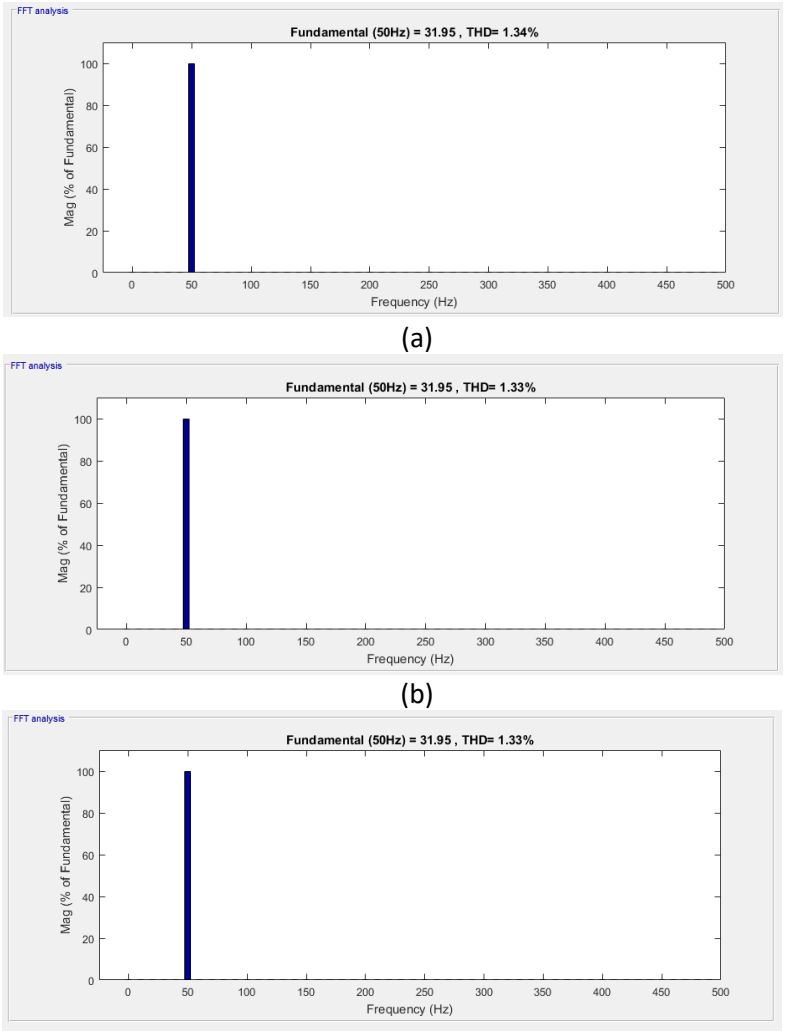

Fig.10. Waveform and FFT Analysis for Line Current (a) Phase A, (b) Phase B, and (c) Phase C

Table 5
THD Analysis for GCPV-DSTATCOM based HCGBP under Non-Linear Load in Load Balancing Condition

Phase	THD (%)	
	Line Current	Load Current
Phase A	1.34	30.86
Phase B	1.33	30.87
Phase C	1.33	30.87

Table 6
Comparison Performance of GCPV-DSTATCOM between PQ theory and HCGBP under Non-Linear load in Steady-State and Load Balancing Conditions

Phase	THD (%)			
	Steady-State		Load Balancing	
	PQ Theory	HCGBP	PQ Theory	HCGBP
Phase A	4.62	1.32	4.62	1.34
Phase B	4.58	1.34	4.58	1.33
Phase C	4.56	1.34	4.56	1.33

4. Conclusion

The growing use of nonlinear loads in power systems has led to an increase in harmonic disturbances and power quality issues. To address these challenges, one approach is to employ DSTATCOM for mitigating current harmonics in distribution systems. This paper presents the use of a GCPV-based DSTATCOM topology with a Hybrid Conjugate Gradient Back Propagation Neural Network (HCGB) based PQ theory control algorithm. The result simulation demonstrates that the proposed GCPV-based DSTATCOM topology with HCGB control algorithm effectively eliminates harmonic currents, and the Total Harmonic Distortion (THD) values of line currents align with the IEEE-519:2014 standard under conditions of non-linear loads in steady-state and load balancing.

Acknowledgement

The author would like to acknowledge the support from the Fundamental Research Grant Scheme (FRGS) under a grant number of FRGS/1/2020/TK0/UNIMAP/02/113 from the Ministry of Education Malaysia.

References

[1] M. Dongare and M. Kalgunde, "Mitigation of Lower Order Harmonics in a Grid-Connected Single-Phase PV Inverter using Shunt Active Filter," in 2017 International Conference on Current Trends in Computer, Electrical, Electronics and Communication (CTCEEC), Sep. 2017, pp. 192-197, doi: 10.1109/CTCEEC.2017.8455001. https://doi.org/10.1109/CTCEEC.2017.8455001

[2] A. B. Taha and S. F. Babiker, "Irradiance Variation Effect on the Electrical Performance of a Grid Connected PV System," in 2019 International Conference on Computer, Control, Electrical, and Electronics Engineering (ICCCEEE), Sep. 2019, vol. 45, no. 15-16, pp. 1-4, doi: 10.1109/ICCCEEE46830.2019.9071427. https://doi.org/10.1109/ICCCEEE46830.2019.9071427

[3] N. D. Tuyen and G. Fujita, "PV-Active Power Filter Combination Supplies Power to Nonlinear Load and Compensates Utility Current," IEEE Power Energy Technol. Syst. J., vol. 2, no. 1, pp. 32-42, 2015, doi: 10.1109/JPETS.2015.2404355. https://doi.org/10.1109/JPETS.2015.2404355

[4] A. Chatterjee and K. B. Mohanty, "Current control strategies for single phase grid integrated inverters for photovoltaic applications-a review," Renew. Sustain. Energy Rev., vol. 92, no. November 2017, pp. 554-569, Sep. 2018, doi: 10.1016/j.rser.2018.04.115. https://doi.org/10.1016/j.rser.2018.04.115

[5] P. Shukl and B. Singh, "Neural Network Based Control Algorithm for Solar PV Interfaced System," in 2019 IEEE Energy Conversion Congress and Exposition (ECCE), Sep. 2019, pp. 2552-2559, doi: 10.1109/ECCE.2019.8912238. https://doi.org/10.1109/ECCE.2019.8912238

[6] X. Liang, "Emerging Power Quality Challenges Due to Integration of Renewable Energy Sources," IEEE Trans. Ind. Appl., vol. 53, no. 2, pp. 855-866, 2017, doi: 10.1109/TIA.2016.2626253. https://doi.org/10.1109/TIA.2016.2626253

[7] K. N. Nwaigwe, P. Mutabilwa, and E. Dintwa, "An overview of solar power (PV systems) integration into electricity grids," Mater. Sci. Energy Technol., vol. 2, no. 3, pp. 629-633, 2019, doi: 10.1016/j.mset.2019.07.002. https://doi.org/10.1016/j.mset.2019.07.002

[8] S. Devassy and B. Singh, "Modified pq-Theory-Based Control of Solar-PV-Integrated UPQC-S," IEEE Trans. Ind. Appl., vol. 53, no. 5, pp. 5031-5040, Sep. 2017, doi: 10.1109/TIA.2017.2714138. https://doi.org/10.1109/TIA.2017.2714138

[9] R. Belaidi, A. Haddouche, D. Ghribi, and M. Mghezzi Larafi, "A Three-Phase Grid-Connected PV System Based on SAPF for Power Quality Improvement," TELKOMNIKA (Telecommunication Comput. Electron. Control., vol. 15, no. 3, p. 1003, Sep. 2017, doi: 10.12928/telkomnika.v15i3.5439. https://doi.org/10.12928/telkomnika.v15i3.5439

[10] R. Kumar, R. Kumar, S. Marwaha, and B. Singh, "S-Transform Based Detection of Multiple and Multistage Power Quality Disturbances," in 2020 IEEE 9th Power India International Conference (PIICON), Feb. 2020, pp. 1-5, doi: 10.1109/PIICON49524.2020.9112945. https://doi.org/10.1109/PIICON49524.2020.9112945

[11] S. H. and S. Shankar, "Study of Power Quality Issues in Wind Distributed Generation System," in 2017 International Conference on Current Trends in Computer, Electrical, Electronics and Communication (CTCEEC), Sep. 2017, pp. 664-668, doi: 10.1109/CTCEEC.2017.8455181. https://doi.org/10.1109/CTCEEC.2017.8455181

[12] O. Koduri, S. S. Duvvuri, and S. D. K. Varma, "A Novel Passive Islanding Detection Methods Using Wavelet Transform for Grid Connected PV System," in 2018 IEEE 13th International Conference on Industrial and Information Systems (ICIIS), Dec. 2018, no. 978, pp. 422-426, doi: 10.1109/ICIINFS.2018.8721382. https://doi.org/10.1109/ICIINFS.2018.8721382

[13] M. R. V. Murali, K. Srinivasu, and L. V. Narasimha Rao, "Enhancement of Power Quality with ANFIS controlled DSTATCOM in four wire three phase distribution system," in 2016 Biennial International Conference on Power and Energy Systems: Towards Sustainable Energy (PESTSE), Jan. 2016, no. 1, pp. 1-8, doi: 10.1109/PESTSE.2016.7516416. https://doi.org/10.1109/PESTSE.2016.7516416

[14] Fang Zheng Peng and Jih-Sheng Lai, "Generalized instantaneous reactive power theory for three-phase power systems," IEEE Trans. Instrum. Meas., vol. 45, no. 1, pp. 293-297, 1996, doi: 10.1109/19.481350. https://doi.org/10.1109/19.481350

[15] Y. W. Li and J. He, "Distribution System Harmonic Compensation Methods: An Overview of DG-Interfacing Inverters," IEEE Ind. Electron. Mag., vol. 8, no. 4, pp. 18-31, Dec. 2014, doi: 10.1109/MIE.2013.2295421. https://doi.org/10.1109/MIE.2013.2295421

[16] S. Kim, Gwonjong Yoo, and Jinsoo Song, "A bifunctional utility connected photovoltaic system with power factor correction and UPS facility," in Conference Record of the Twenty Fifth IEEE Photovoltaic Specialists Conference - 1996, 1996, pp. 1363-1368, doi: 10.1109/PVSC.1996.564386. https://doi.org/10.1109/PVSC.1996.564386

[17] P. S. Sanjan, N. G. Yamini, and N. Gowtham, "Performance Comparison of Single-Phase SAPF Using PQ Theory and SRF Theory," in 2020 International Conference for Emerging Technology (INCET), Jun. 2020, pp. 1-6, doi: 10.1109/INCET49848.2020.9154126. https://doi.org/10.1109/INCET49848.2020.9154126

[18] M. Iqbal et al., "Neural Networks Based Shunt Hybrid Active Power Filter for Harmonic Elimination," IEEE Access, vol. 9, pp. 69913-69925, 2021, doi: 10.1109/ACCESS.2021.3077065. https://doi.org/10.1109/ACCESS.2021.3077065

[19] L. N. Li, X. F. Liu, F. Yang, W. M. Xu, J. Y. Wang, and R. Shu, "A review of artificial neural network based chemometrics applied in laser-induced breakdown spectroscopy analysis," Spectrochimica Acta - Part B Atomic Spectroscopy, vol. 180, no. November 2020. Elsevier B.V., p. 106183, 2021, doi: 10.1016/j.sab.2021.106183. https://doi.org/10.1016/j.sab.2021.106183

[20] A. Surendran M. and P. Baburai, "A Comparison Study of Optimization Based PI Controller Tuning for PQ Improvement in DSTATCOM," in 2019 2nd International Conference on Intelligent Computing, Instrumentation and Control Technologies (ICICICT), Jul. 2019, pp. 179-184, doi: 10.1109/ICICICT46008.2019.8993407. https://doi.org/10.1109/ICICICT46008.2019.8993407

[21] U. R. Babu, V. V. K. Reddy, and S. T. Kalyani, "Power quality improvement in RDS using smart DSTATCOM," in Asia-Pacific Power and Energy Engineering Conference, APPEEC, 2018, vol. 2017-Novem, pp. 1-6, doi: 10.1109/APPEEC.2017.8308966. https://doi.org/10.1109/APPEEC.2017.8308966

[22] H. K. Yada and M. S. R. Murthy, "An improved control algorithm for DSTATCOM based on single-phase SOGI-PLL under varying load conditions and adverse grid conditions," in IEEE International Conference on Power Electronics, Drives and Energy Systems, PEDES 2016, Dec. 2017, vol. 2016-Janua, pp. 1-6, doi: 10.1109/PEDES.2016.7914564. https://doi.org/10.1109/PEDES.2016.7914564

[23] M. P. Kazmierkowski, "Power Quality: Problems and Mitigation Techniques [Book News]," IEEE Ind. Electron. Mag., vol. 9, no. 2, pp. 62-62, Jun. 2015, doi: 10.1109/MIE.2015.2430111. https://doi.org/10.1109/MIE.2015.2430111

[24] M. P. Kazmierkowski, "Power Quality: Problems and Mitigation Techniques [Book News]," IEEE Ind. Electron. Mag., vol. 9, no. 2, pp. 62-62, Jun. 2015, doi: 10.1109/MIE.2015.2430111. https://doi.org/10.1109/MIE.2015.2430111

[25] S. Devassy and B. Singh, "Design and Performance Analysis of Three-Phase Solar PV Integrated UPQC," IEEE Trans. Ind. Appl., vol. 54, no. 1, pp. 73-81, 2018, doi: 10.1109/TIA.2017.2754983. https://doi.org/10.1109/TIA.2017.2754983

[26] O. P. Mahela and A. G. Shaik, "A review of distribution static compensator," Renew. Sustain. Energy Rev., vol. 50, pp. 531-546, 2015, doi: 10.1016/j.rser.2015.05.018. https://doi.org/10.1016/j.rser.2015.05.018

[27] J. Jayachandran and R. Murali Sachithanandam, "Neural Network-Based Control Algorithm for DSTATCOM Under Nonideal Source Voltage and Varying Load Conditions," Can. J. Electr. Comput. Eng., vol. 38, no. 4, pp. 307-317, 2015, doi: 10.1109/CJECE.2015.2464109. https://doi.org/10.1109/CJECE.2015.2464109

[28] S. Sinha and A. Arora, "Comparison of IRPT and ANN based Control Algorithm for Shunt Compensation in Grid Connected Systems," in 2021 International Conference on Intelligent Technologies (CONIT), Jun. 2021, pp. 1-5, doi: 10.1109/CONIT51480.2021.9498281. https://doi.org/10.1109/CONIT51480.2021.9498281

[29] B. Singh, A. Adya, A. P. Mittal, and J. R. . Gupta, "Neural Network Based DSTATCOM Controller for Three-phase, Three-wire System," in 2006 International Conference on Power Electronic, Drives and Energy Systems, Dec. 2006, no. Vdc, pp. 1-6, doi: 10.1109/PEDES.2006.344288. https://doi.org/10.1109/PEDES.2006.344288